

## Direct measurement of polarization resolved transition dipole moment in InGaAs/GaAs quantum dots

K. L. Silverman<sup>a)</sup> and R. P. Mirin

*National Institute of Standards and Technology, Boulder, Colorado 80305*

S. T. Cundiff

*JILA, National Institute of Standards and Technology and University of Colorado, Boulder, Colorado 80309*

A. G. Norman

*National Renewable Energy Laboratory, Golden, Colorado 80401*

(Received 2 January 2003; accepted 17 April 2003)

The propagation of optical pulses resonant with the ground-to-excited state transition of InGaAs quantum dots is investigated. An analysis of low intensity excitation yields a dipole moment of  $8.8 \times 10^{-29}$  to  $10.9 \times 10^{-29}$  C m, depending on the quantum dot growth conditions. We observe polarization of the dipole moment exclusively in the plane perpendicular to the growth direction.

© 2003 American Institute of Physics. [DOI: 10.1063/1.1584514]

In the past few years, self-assembled quantum dots (QDs) have been the focus of an intense research effort. This can be attributed to their promise as active regions in optoelectronic devices and as an ideal semiconductor system for studying the physics of two-level systems. The forefront of QD research is applying their atomlike properties to next generation optical devices such as quantum computers and quantum cryptographic systems. There has already been much experimental and theoretical work in this area, but there are surprisingly few results on measuring the strength of the interaction between a self-assembled QD and a light field. Previous measurements of the QD dipole moment were performed by analyzing threshold currents of QD laser diodes.<sup>1</sup> This method relies on a laser model that assumes the Fermi level is pinned above threshold. It is not clear whether this will hold for the strong lateral confinement present in QD active regions.<sup>2</sup> Other methods for measuring the absorption coefficient have suffered from a large uncertainty due to large background absorption,<sup>3</sup> problems estimating coupling efficiency into and out of the dot region,<sup>4,5</sup> or have relied on differential transmission techniques.<sup>6</sup>

In this letter, we directly measure the absorption coefficient of various ensembles of InGaAs/GaAs self-assembled QDs. The measurement involves coupling light into a waveguide containing QDs in the core and time resolving the output. The advantages are increased interaction length with the weakly absorbing QDs and observation of the decay of light pulses over successive cavity round trips. Since waveguide coupling has an equal affect on each pulse exiting the waveguide, the large uncertainty associated with it does not hinder our measurement. We then relate the ensemble properties of the dots to the dipole moment.

The samples were grown by molecular-beam epitaxy on a GaAs substrate and contain a single layer of In<sub>0.45</sub>Ga<sub>0.55</sub>As QDs grown at a substrate temperature of 520 °C. In order to compare dots of different sizes and ground-state energies, the amount of material deposited was different for each of the

samples. The QD layers are buried in a 270 nm Al<sub>0.10</sub>Ga<sub>0.90</sub>As waveguide core clad with Al<sub>0.70</sub>Ga<sub>0.30</sub>As providing optical confinement in the growth direction. To minimize the contribution of free carrier absorption to modal loss, the entire structure is undoped. We wet etched 3 μm wide stripes in the top cladding layer and the waveguide was cleaved, giving a cavity length of approximately 1 mm.

In order to characterize the samples grown for this experiment, we performed low-temperature photoluminescence (PL) and transmission electron microscopy (TEM). At a low temperature, the PL spectra can be used to determine the inhomogeneous broadening of the QD states. In order to perform the TEM measurements on the same sample used in the experiment, we first etched off the top waveguide cladding down to within 100 nm of the QD layer. A (220) dark-field image was taken, showing the strain contrast of the QDs. The TEM images were used to determine the QD areal density. Figure 1 is a sample TEM image.

Figure 2 shows the experimental setup and typical data. Pulses from a synchronously pumped optical parametric oscillator (OPO) are coupled into the waveguides. Light that is

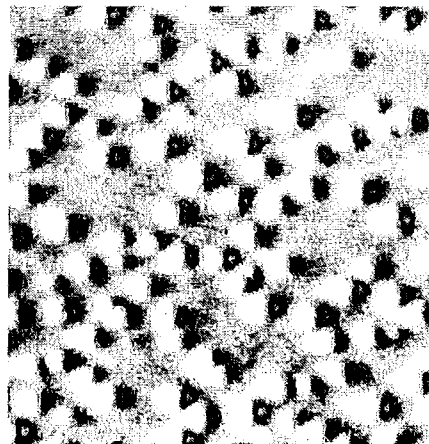
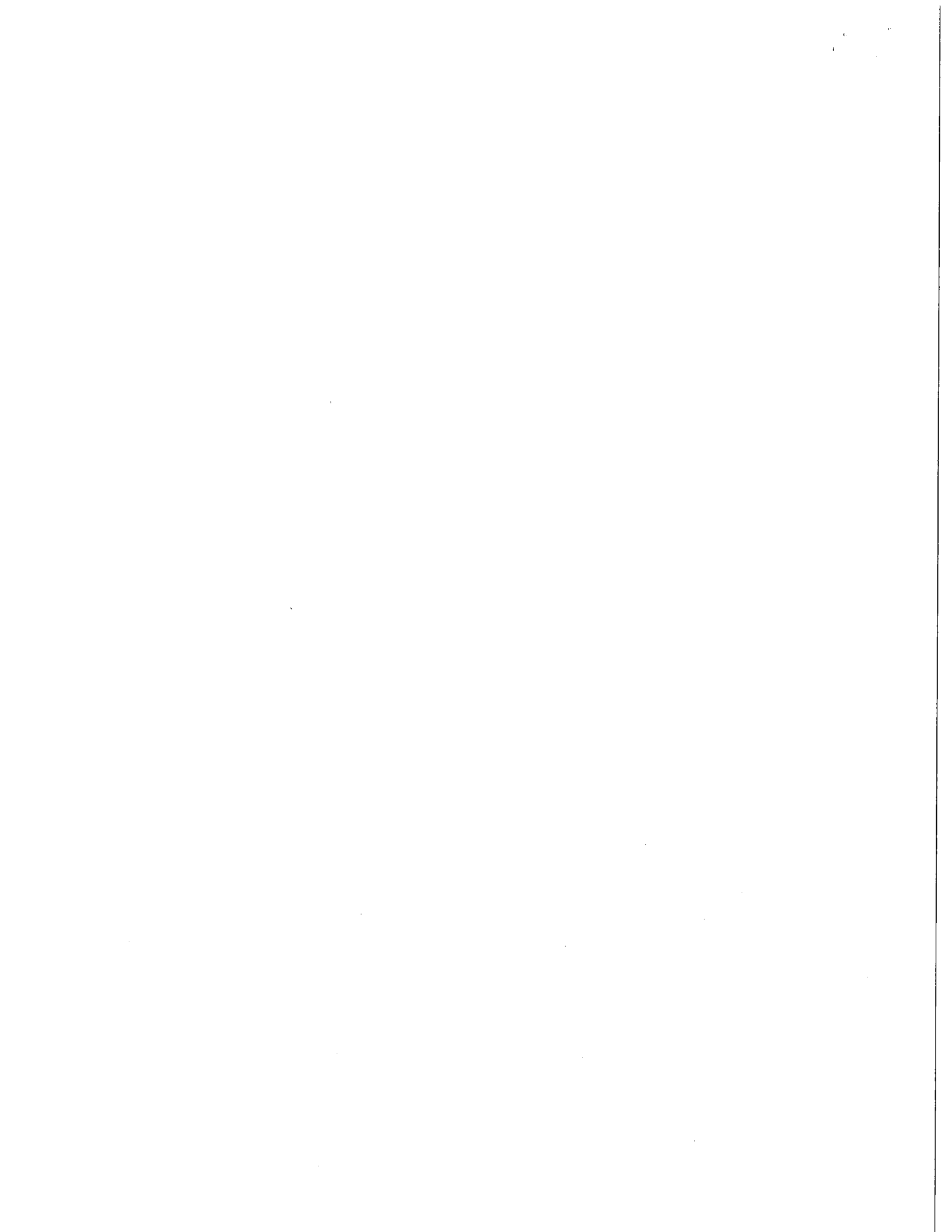


FIG. 1. Top-view TEM image of as grown InGaAs/GaAs QDs. Image field is 500 nm×500 nm.

<sup>a)</sup>Electronic mail: silverma@boulder.nist.gov



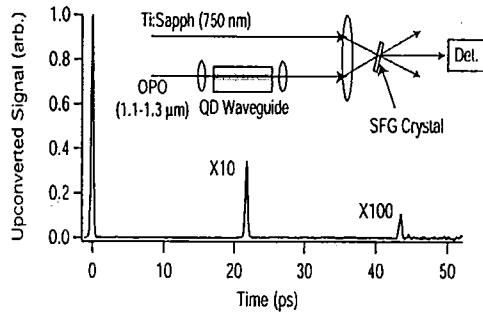


FIG. 2. Experimental setup along with typical data. The pulses have an approximate bandwidth of 12 nm and the nonlinear crystal is 1.5 mm of Beta Barium Borate (BBO).

coupled out of the waveguide is mixed with a gating pulse in a nonlinear crystal. By scanning the delay of the gating pulse, we time resolve the waveguide output. The typical data in Fig. 2 shows the temporal profile of the OPO pulse that traversed the waveguide once, as well as two reflections from the cleaved waveguide facets. The pulse at 22 ps makes one additional round trip and the pulse at 44 ps makes two additional round trips.

By comparing the area of the first pulse to that which makes one additional round trip, we directly determined the absorption coefficient by

$$\int I_i(t) dt = R_{TE, TM}^2 \exp^{-\alpha 2L} \int I_{i-1}(t) dt, \quad (1)$$

where  $I$  is the pulse intensity,  $R_{TE, TM}$  is the facet reflectivity for the transverse electric (TE) or transverse magnetic (TM) waveguide mode,  $\alpha$  is the absorption coefficient, and  $L$  is the length of the device.  $R_{TE, TM}$  was determined from measurements on empty waveguides of various lengths to be 0.34 and 0.21, respectively, for the TE and TM modes. From the same measurements, we were also able to determine that the background waveguide loss was less than  $0.3 \text{ cm}^{-1}$  over most of the experimental wavelength range. As the wavelength approaches  $1.3 \text{ }\mu\text{m}$ , background loss becomes appreciable, particularly in the TM optical mode. This background loss only affected our longest wavelength sample (B453) and the data were corrected accordingly.

To make certain we were operating in a regime where Eq. (1) correctly describes the loss of pulse energy, we performed intensity-dependent loss measurements. Figure 3 shows TE mode loss determined using Eq. (1) on data collected from sample B453. Three regimes of pulse propagation are clearly evident. Below  $100 \text{ }\mu\text{W}$ , we are in the linear pulse propagation regime and Eq. (1) correctly describes the

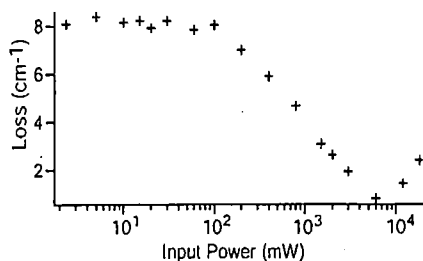


FIG. 3. TE loss vs input power.

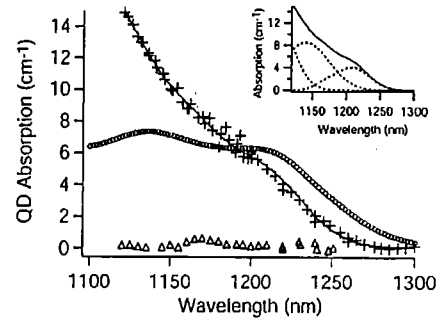


FIG. 4. Measured QD absorption of the TE (+) and TM ( $\Delta$ ) waveguide mode for sample B453. Included on the main graph is the room-temperature PL spectrum ( $\circ$ ) and a least-squares fit to the TE absorption data (solid line). Inset: Breakdown of individual peaks making up best fit.

loss of pulse energy per pass due to QD absorption. Above  $100 \text{ }\mu\text{W}$ , saturation begins to set in as the QD states become filled and the loss begins to decrease. Above  $6 \text{ mW}$ , two-photon absorption in the waveguide core becomes dominant and the loss begins to increase. All further data presented are collected in the linear pulse propagation regime.

Experimental TE and TM absorption data for our longest-wavelength sample are shown in Fig. 4. We have also included the room-temperature PL spectrum for comparison. The TM absorption for this sample is at the noise floor of our measurement. The absence of TM ground-state absorption has been demonstrated by other authors, but here we can say that it is less  $0.3 \text{ cm}^{-1}$ . In addition, we see no TM absorption in any of the excited states in our sample. This differs from the results in Ref. 5, but may be attributable to the pyramidal shape of our dots. Also, the fact that our sample contains only a single QD layer precludes any vertical coupling between QDs. Vertical dot coupling can change the symmetry of the wave function, allowing a non-zero dipole moment in the growth direction.<sup>7</sup> We would expect this effect to be strongest in the QD excited states, due to their weaker confinement.

Included in Fig. 4 is a least-squares fit to our experimental data. We determined the lineshape of the QD ground and excited states from low-temperature PL. Our fitting parameters included peak heights and positions. In this way, we isolated the contribution of the ground state to the absorption curve. We then used the ground-state absorption spectrum, along with the QD areal density determined from TEM images in order to calculate the transition dipole moments. Under the assumption that inhomogeneous broadening dominates in our QD linewidth, we used the following equation to calculate the dipole moment ( $\mu_{cv}$ ):

$$\mu_{cv}^2 = 12.6 \left( \frac{\Delta\lambda}{\lambda_0} \right) \left( \frac{\alpha_0 V}{N} \right), \quad (2)$$

where  $\alpha_0$  is the absorption peak in  $\text{cm}^{-1}$ , and  $V/N$  is the effective density of QDs that takes into account the aerial density ( $N_{2D}$ ) and the transverse confinement factor. The results for the three samples measured are given in Table I. We estimate that the largest source of uncertainty in our dipole moment measurements is the uncertainty in  $N_{2D}$  ( $\approx \pm 15\%$ ).

TABLE I. Results:  $\lambda_0$  is the center wavelength of the ground-state transition and  $\Delta\lambda$  is the FWHM of the ground-state transition.

Sample	$N_{2D}$ ( $\text{cm}^{-2}$ )	$\lambda_0$ (nm)	$\Delta\lambda$ (nm)	$\alpha_{\text{max}}$ ( $\text{cm}^{-1}$ )	Dipole moment [C m (Debye)]
B429	$3.7 \times 10^{10}$	1123	56	6.3	$10.4 \times 10^{-29}$ (31.2)
B430	$3.9 \times 10^{10}$	1151	54	5.1	$8.8 \times 10^{-29}$ (26.4)
B453	$1.9 \times 10^{10}$	1210	60	3.8	$10.9 \times 10^{-29}$ (32.6)

The results in Table I show no dependence of the dipole moment on transition energy or dot density within our level of uncertainty. It has been predicted that the dipole moment should increase as the square root of QD area due to increased coupling to the light field<sup>8</sup> for the case of QDs with a height much smaller than the base. Although longer-wavelength dots have a larger height, it is unclear whether they necessarily have a larger base diameter. Without high-resolution TEMs on these structures, we do not know whether or not to expect a change in dipole moment with transition energy. Also, note that the dipole moment of sample B430 is significantly smaller than the others. This sample exhibited an extremely wide first-excited state [full width at half maximum (FWHM)  $\approx 100$  nm] that may indicate a very different dot shape than the other two samples.

It is interesting to compare our results with other measurements in literature. They are consistent with the results ( $\mu_{cv} = 29.3$  Debye) obtained by analyzing threshold currents

of QD laser diodes.<sup>1</sup> This suggests that their assumption of Fermi-level pinning is a good one for their structure. When comparing our results with those of Borri *et al.*,<sup>4,9</sup> there is good agreement with their small-signal measurements (30 Debye) but poor agreement with their measurements of Rabi oscillations (19 Debye). The large discrepancy between the value obtained by Rabi oscillations and our results is most likely associated with difficulties in estimating the electric-field strength in the QD region.

In conclusion, we have measured the dipole moment of single-layer InGaAs/GaAs QDs to be 26 to 33 Debye, depending on growth conditions. Our dots show no TM optical absorption through the second-excited state transition.

<sup>1</sup>P. G. Elisee, H. Li, A. Stintz, G. T. Liu, T. C. Newell, K. J. Malloy, and L. F. Lester, Appl. Phys. Lett. 77, 262 (2000).

<sup>2</sup>M. Sugawara, K. Mukai, and Y. Nakata, Appl. Phys. Lett. 74, 1561 (1999).

<sup>3</sup>P. M. Smowton, E. Herrmann, Y. Ning, H. D. Summers, and P. Blood, Appl. Phys. Lett. 78, 2629 (2001).

<sup>4</sup>P. Borri, W. Langbein, S. Schneider, U. Woggon, R. L. Sellin, D. Ouyang, and D. Bimberg, Phys. Rev. B 66, 081306 (2002).

<sup>5</sup>S. Cortez, O. Krebs, P. Voisin, and J. M. Gerard, Phys. Rev. B 63, 233306 (2001).

<sup>6</sup>D. Birkedal, J. Bloch, J. Shah, L. N. Pfeiffer, and K. West, Appl. Phys. Lett. 77, 2201 (2000).

<sup>7</sup>L. Chu, M. Arzberger, A. Zrenner, G. Bohm, and G. Abstreiter, Appl. Phys. Lett. 75, 2247 (1999).

<sup>8</sup>A. Thranhardt, C. Ell, G. Khitrova, and H. M. Gibbs, Phys. Rev. B 65, 035327 (2002).

<sup>9</sup>P. Borri, E. Langbein, J. M. Hvam, F. Heinrichsdorff, M.-H. Mao, and D. Bimberg, IEEE J. Sel. Top. Quantum Electron. 6, 544 (2000).